

# *Medical Image Fusion Method Based on NSCT with SR in Frequency Partition Domain*

*C. Rama Mohan<sup>1</sup>, Kanamukkala Anusha<sup>2</sup>, Gunnam reddy Amritha reddy<sup>3</sup>, Arava Gowthami<sup>4</sup>, Peramana HariPriya<sup>5</sup>*

*Assistant Professor<sup>1</sup>, U.G Scholar<sup>2,3,4,5</sup> Department of Computer Science and Engineering*

*E-mail: ramamohanc@yahoo.com<sup>1</sup>, anushakanamukkala@gmail.com<sup>2</sup>, amrithareddy@gmail.com<sup>3</sup>, aravagouthamy123@gmail.com<sup>4</sup>, hariharipriya999@gmail.com<sup>5</sup>*

*Narayana Engineering College, Nellore, India*

## **Abstract:**

The visual impact of medical images is very important for a clinical assistant diagnosis. Medical image fusion methods can incorporate data from various medical images to obtain an informative image that is better suited for joint diagnosis, preoperative planning, intraoperative instruction and interventional therapy. For reducing the noise, first of all, both medical images are converted into the domain of frequency partition (FP). So, the subband components of row and column components are obtained. Then, fuse the row and column components separately using average fusion rule and perform the Nonsubsampled Contourlet Transform on row & column components fused images to get the frequency coefficients respectively. The low and high frequency components are fused using Sparse Representation. Finally, by performing the inverse NSCT on the merged components the fused image is obtained. The suggested technique of fusion is evaluated on a variety of medical images and contrasted to several common techniques of image fusion. The experimental results show that in terms of subjective quality and objective assessment, the proposed fusion method can provide better fusion results.

**Keywords:** Image Fusion, Nonsubsampled Contourlet Transform, Sparse Representation, Frequency Partition, Quality Evolution Metrics, Image Quality

## **Introduction**

Multi-sensor image fusion (MIF)[1] has developed in today's world as an groundbreaking and exciting scientific field of image processing, with a range of uses varying from defense, weather forecasting, computer vision, robotics, security, improved visual field machine, and radiography, etc.[2]. The idea is that two or

more recorded images are composed of this methodology. This process allows the spatial resolution of acquired low-detailed multisensor images to be increased and thus retains their spectral details. With a lot of advanced techniques and methods the field of medical imaging is growing rapidly. For high-performance technologies including X-rays, the modalities of nuclear imaging, MRI,

and ultrasound have evolved. Such images thus obtained remain today as the most important diagnostic instruments in medicine. The sensors used in the imaging process are very specific and provide a very important component of acquisition. A single sensor could not be adequate to provide an all-inclusive view of the environment under interest. For the best diagnostic & therapeutic reason, multimodal medical imaging is the way forward [3].

## 2. Discrete Cosine Transform (DCT)

Discrete Cosine Transform [4 - 6] is commonly used and accepted within the field of image processing. The DCT coefficients concentrate on the low-frequency field. High frequency coefficients make an excellent contribution to energy compactness and edges. DCT uses cosine waves which change the data of the image. After the decorrelation method, the DCT coefficients are encoded independently without losing the compression efficiency. DCT is strictly actual compared to DFT, and has various uses for science and engineering. DCT methodology utilizes spectral methods for numerical solutions to partial differential equation.

### Limitations of Discrete Cosine Transform

- Higher spectral coefficients cause DCT to become blurred.
- In the case of quantization, some low spectral coefficients cause compression artifacts in smooth portions of the image.
- Block boundaries consist of DCT artifact blocking sequence as each block

is encoded with various strategies and external quantization.

## 3. Proposed Method

The proposed system structure is shown in Figure 1, which involves three processes: the FPDCT-based image fusion process, Nonsubsampled Contourlet Transform (NSCT) and Sparse Representation (SR) process. The three steps are below. The NSCT-SR in Frequency Partition based image fusion is defined in Algorithm 1.

**Algorithm 1:** NSCT\_SR\_FP based image fuse

**Input:** Medical Images

**Output:** Fused Image

**Steps:**

1. Start
2. Load the source images
3. Perform the frequency partition on source image A & source image B to get the row and column components respectively.
4. Perform the image fusion for the row and column components separately using average fusion rule
5. Perform the Nonsubsampled Contourlet Transform (NSCT) on row & column components fused images to get the frequency coefficients respectively.
6. Fuse the frequency coefficients with Sparse Representation.
7. Perform the inverse Nonsubsampled Contourlet Transform on the composite component to obtain the composited image i.e., fused image.
8. Stop

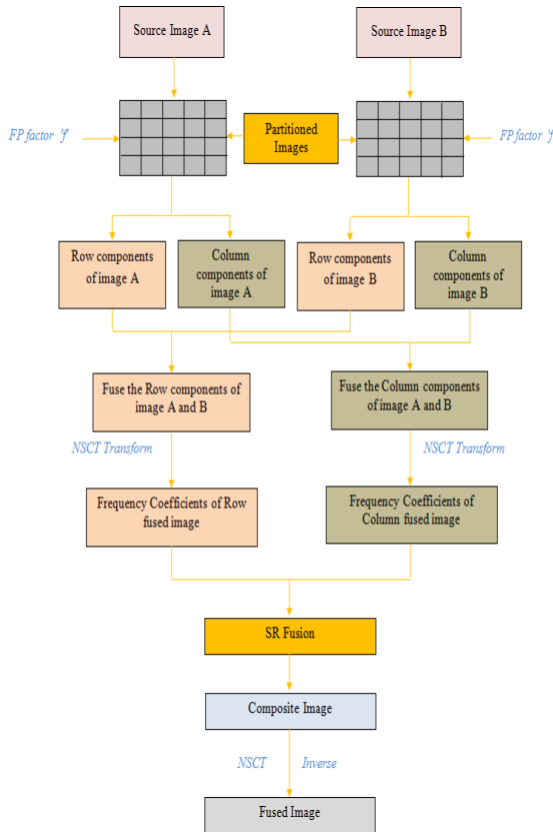


**Figure 1:** The flow diagram of proposed method

**3. 1. Frequency Partition**

The FPDCT-based image fusion [7 - 11 ] is defined in Algorithm 1, for merging row and column components with a partition factor 'f'. Detailed explanation of such important techniques and algorithms is as follows.

Frequency is a periodic motion undergone for one cycle after passing through series of values. Frequency partition refers to identification of RC and CC in given set of data. Further apply frequency function f which divides RC and CC values separately. The row components is shown here by the RC and the column component by the CC shows. Frequency partition is used to reduce the noise of an image. With the help of 1D

DCT, vector data has been generated with DCT function  $Z(x)$ . Further, DCT coefficients are identified for the given vector. The DCT coefficients fall into two groups: components with row and components with column. For energy compaction DCT coefficients, a partition factor 'f' is added that distinguishes DCT coefficients with a row and a column frequency as illustrated below.

$$A(p) = DCT(a(p)), p, v = 0,1,2, \dots, XY - 1 \tag{1}$$

$$AL(v) = A(v), v = 0,1,2, \dots, XYf - 1 \tag{2}$$

$$A(v) = A(v), v = XYf, XYf + 1, \dots, XY - 1 \tag{3}$$

Let the images to be fused are  $a_1(p,q)$  &  $a_2(p,q)$  and the image fusion process is as follows:

$$a_1(p) = c2dt1d(a_1(p, q), X, Y) \tag{4}$$

$$a_2(p) = c2dt1d(a_2(p, q), X, Y) \tag{5}$$

$$A_1(v) = DCT(a_1(p)) \tag{6}$$

$$A_2(v) = DCT(2(p)) \tag{7}$$

Using eq. 3, the fused coefficients are:

$$AL_f(v) = 0.5(AL_1(v) + AL_2(v)), v = 0,1, \dots, XYf - 1 \tag{8}$$

$$AH_f(v) = \begin{cases} AH_1(v) & \text{if } |AH_1(v)| \geq |AH_2(v)| \\ AH_2(v) & \text{if } |AH_1(v)| < |AH_2(v)| \end{cases}, v = XYf, XYf + 1, \dots, XY - 1 \tag{9}$$

$$A_f(v) = [AL_f(v)AH_f(v)] \quad (10)$$

$$a_f(p) = \text{idct}(A_f(v)), \quad p, v \\ = 0, 1, 2, \dots, XY - 1 \quad (11)$$

The fused image is:

$$I_f = \text{c1dt2d}(A_f(p), X, Y) \quad (12)$$

Where the subscript 1 or 2 or f indicates 1<sup>st</sup> or 2<sup>nd</sup> or fused image respectively.

### 3. 2. Nonsubsampled Contourlet Transform (NSCT)

NSCT [12] overcomes the drawbacks of wavelet and Contourlet transforms. It has the benefits of multiscale and multidirectional analysis, and invariance of translation and anisotropy [3]. The NSCT transformation consists of two steps: the decomposition of the non-downsampling pyramid (NSP) and the filter bank (NSDFB) for the non-downsampling path. NSP decomposition is the method of decomposing the source image into subbands of low and high frequency via the filter bank of the nonsampling tower to ensure the characteristic of multiscale NSCT transformation.

### 3. 3. Sparse Representation (SR)

Sparse Representation [13] can extract deeper structural characteristics between coefficients of low frequency subbands and express or approximate them in a linear combination of a few atoms [14]. Sparse representation (SR) has proved to be an extremely powerful method for analyzing high-dimensionality signals [15], so SR to the field of image fusion for better fused outcomes [16–21].

## 4. The Results and Analysis of Experiments

The medical image test pairs (CT / MRI, MR - T1 / MR - T2, MR - PD / MR - T2, MR - T1 / MR - T2, and MR - PD / MR - T2) were chosen by online resources such as <http://www.med.harvard.edu/AANLIB/home.html> page. These images were given as inputs for different standard fusion algorithms such as SR, DTCWT, CVT, NSCT, and NSCT-SR and NSCT-SR + Frequency Partition (proposed method). The performance of these algorithms was analyzed using different visual and quantitative measures. The proposed algorithm fuse source images with NSCT-SR + Frequency Partition process to reduce the noise and recover the resolution losses.

Different statistical measures [22 - 26] such as Information Entropy (IE), Mean (API), Standard Deviation (SD), Spatial Frequency (SF), edge information delivery factor ( $Q^{AB/F}$ ), Mean Gradient (AG) used to quantify the performance of the fusion algorithms mentioned. The computed values of the statistical measures for different standard image test pairs using the mentioned fusion algorithms are specified in the table 1- 5. Based on the nature of these statistical measures, the values of IE, API, SD, SF,  $Q^{AB/F}$ , and AG should be of higher value to show the enhanced performance of the fusion algorithm. The images obtained after fusion process should be in such a way that it provide more necessary information based on people's perceptions, visual and quantitative analysis. The visual analysis of the fused image should reveal the significant

improvement in the transfer of information from the source images, information lost from the source images and less artifacts.

Figure 2 describes the original CT / MRI images obtained by different image fusion algorithms. The image (figure 2(h)) obtained from the proposed fusion algorithm shows better visual quality and less information loss. The statistical metrics evaluated for original CT / MRI images using different fusion algorithms are specified in the table 1. After the comparison of the statistical measures obtained by different fusion algorithms, the proposed method shows good performance over other standard fusion methods.

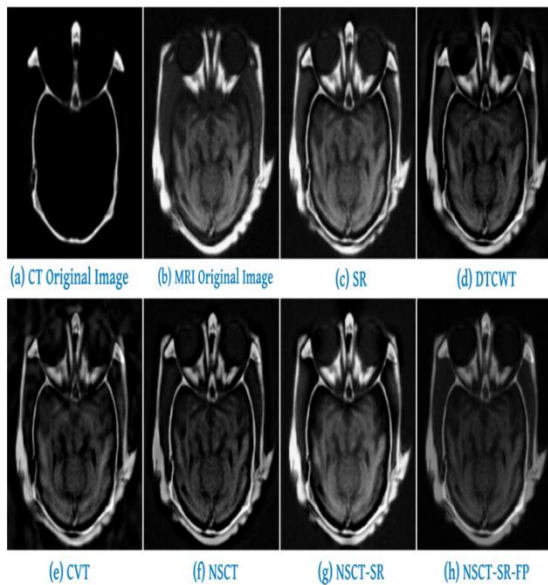


**Figure 2: Medical Images (CT / MRI) fusion outcomes**

The original MR - PD / MR - T1 images and images after various image fusion methods can be visualized in Figure 3. After the visual analysis of these images, the image

from the source images, information lost. obtained using the proposed method shows better quality and less information loss.

Table 2 shows the statistical measures of the different fusion algorithms and the metrics obtained for the proposed algorithm shows better values than compared to other algorithms.

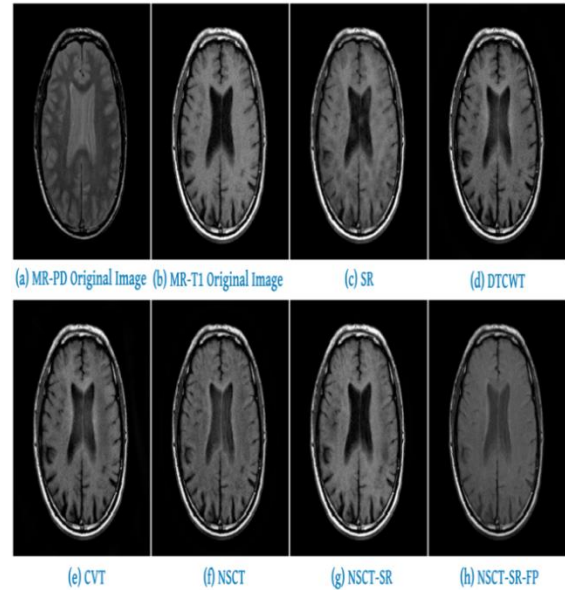


**Figure 3: Medical Images (MR - PD / MR - T1) fusion outcomes**

Original medical MR - PD / MR - T2 images obtained after applying to different fusion algorithms are shown in figure 4. The boat image (figure 4(h)) obtained using the proposed method shows the better visual appearance and appreciably more image quality. Table 3 shows the quality metrics of the MR - PD / MR - T2 image using different fusion algorithms. From the visual appearance and quality metrics the proposed algorithm shows better performance than other algorithms.



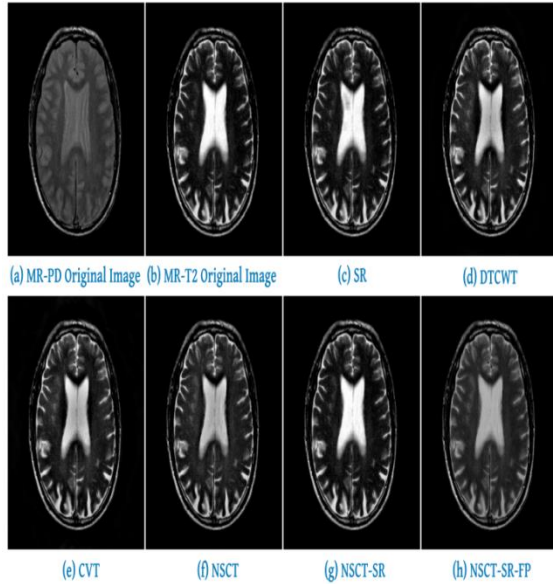


**Figure 4:** Medical Images (MR - PD / MR - T2) fusion outcomes

The visual information of medical MR - T1 / MR - T2 images both input and output of various image fusion algorithms are shown in figure 5. Table 4 gives the statistical measures of the fusion algorithms of the medical MR - T1 / MR - T2 image. After comparing the performance of the fusion methods, the proposed method shows good image quality and better statistical measures.

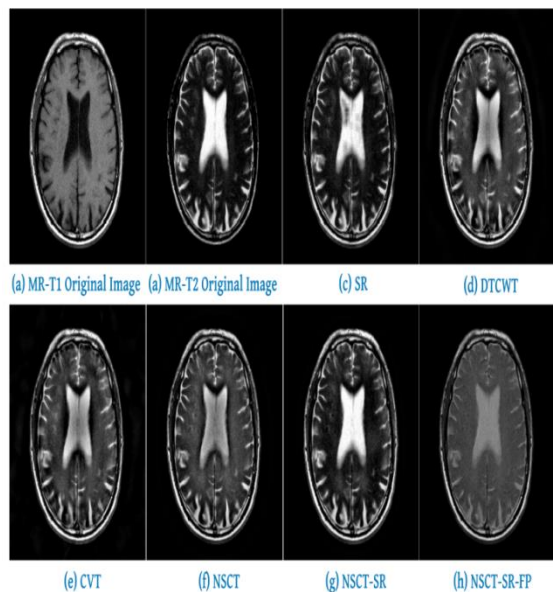


**Figure 5:** Medical Images (MR - T1 / MR - T2) fusion outcomes

Figure 6 shows the medical MR - PD / MR - T2 images of various fusion algorithms. The fusion image obtained using proposed method shows better visual quality and appreciably no loss of information. Table 5 gives the information about statistical measures of the MR - PD / MR - T2 image processed with different image fusion algorithms. The comparison of the processed fusion images and statistical measures reveals that the proposed method shows better performance than other algorithms.

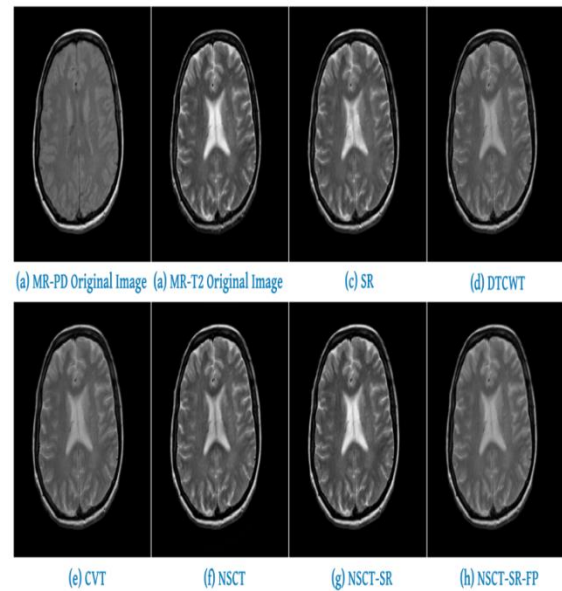


**Figure 6:** Medical Images (MR - PD / MR - T2) fusion outcomes

The medical images are mentioned with notation IDS1 to IDS5. The statistical measures obtained with different fusion methods for different medical images are plotted for analysis. Figure 7 shows the variation of the metrics IE and API for the different medical images processed with fusion algorithms. The highest values of

these metrics indicate the better performance of the image fusion algorithm. The proposed method shows highest values among the other fusion methods and in turn shows good efficiency.

fusion methods for all the medical image sets. In view of this result the proposed fusion algorithm outperforms and shows best performance than comparing to other algorithms.

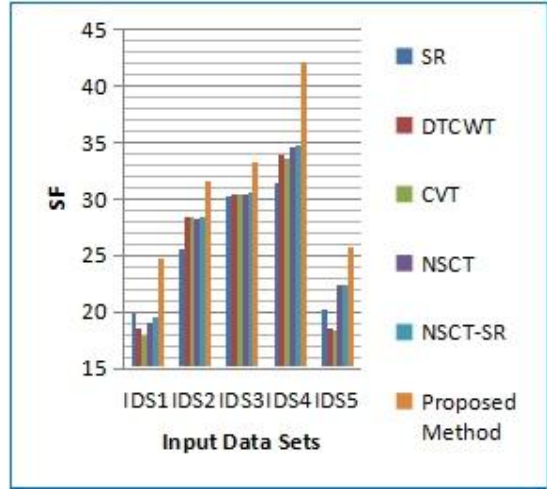
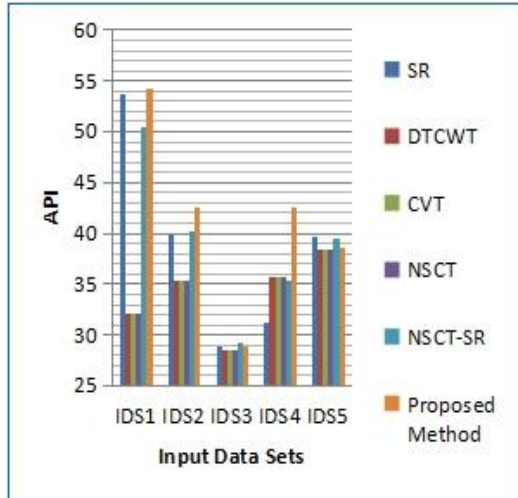
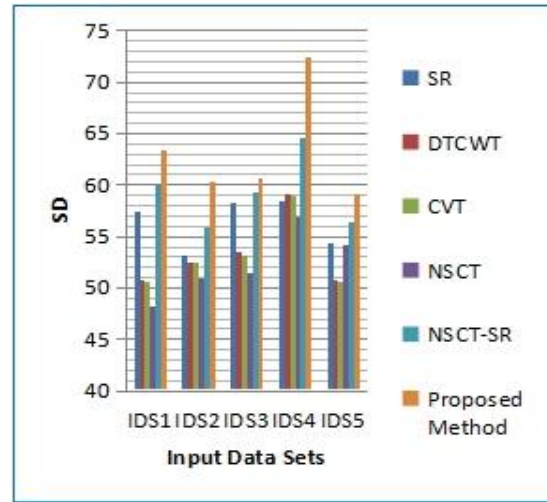
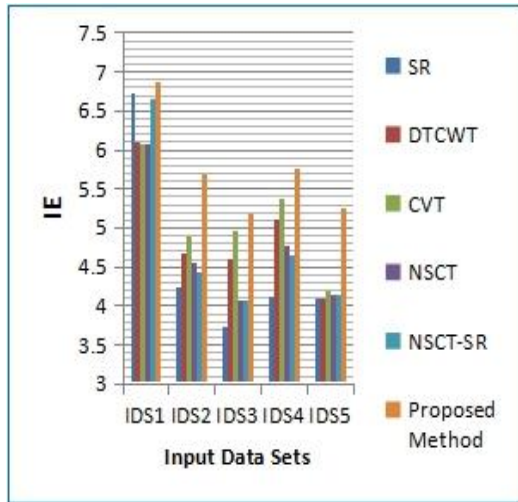


**Figure 7: Quality metrics (IE and API) comparison for medical image sets.**

**Figure 8: Quality metrics (SD and SF) comparison for medical image sets.**

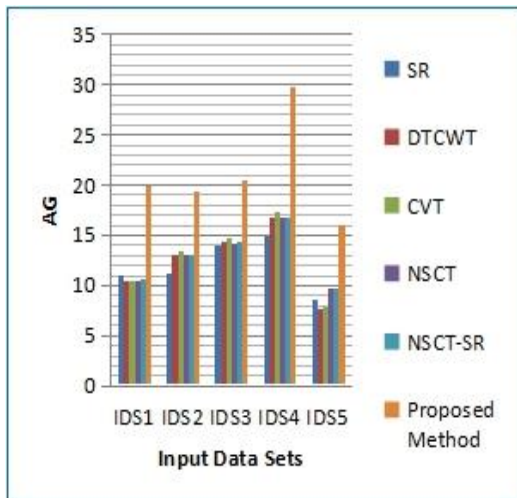
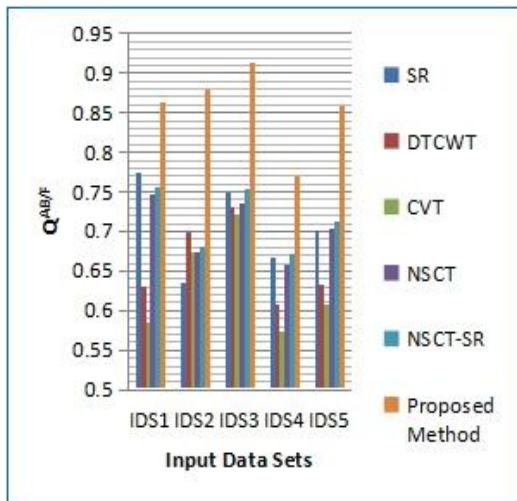
Similarly, figure 8 shows the variation of SD and SF quality metrics. The proposed method shows better high value of SD and high value of SF than comparing to other

The variation of statistical measures such as  $Q^{AB/F}$  and AG for different images is shown in figure 9. The figure reveals the highest value of  $Q^{AB/F}$  (optimal value) for all

medical image sets. The AG parameter obtained by the proposed method for all the medical images shows with highest value (optimal value). From the comparison of these statistical metrics for different medical images using different fusion methods, it is evident that the proposed algorithm shows best performance over other fusion algorithms

**Figure 9:** Quality metrics ( $Q^{AB/F}$  and AG) comparison for medical image sets.

The results illustrates that not only the proposed fusion algorithm applied to all six multifocus image sets shows better visual performance but also the statistical measures proved the same than compared to other fusion methods. It is also evidenced that the proposed algorithm shows better visual appearance and also exhibits better statistical measures than compared to other methods published recently [12].





Algorithm	IE	API	SD	SF	Q <sup>AB/F</sup>	AG
SR	4.22767380	39.9013366	53.0800168	25.586103	0.635592793	11.2318891
DTCWT	4.67977447	35.3688125	52.5094439	28.3897179	0.698514784	13.0442014
CVT	4.88452442	35.3688125	52.4634592	28.3639524	0.674880836	13.4343859
NSCT	4.54672433	35.3688125	50.9684416	28.3029146	0.674847285	13.0314584
NSCT-SR	4.44303909	40.1107795	55.9059575	28.4290573	0.680786743	12.9694243
<b>Proposed Method</b>	<b>5.69057281</b>	<b>42.5682135</b>	<b>60.2808145</b>	<b>31.5654012</b>	<b>0.878659328</b>	<b>19.2939626</b>

**Table 2:** Statistical measures of medical images (MR - PD / MR - T1) using different fusion algorithms

Algorithm	IE	API	SD	SF	Q <sup>AB/F</sup>	AG
SR	3.71943182	28.8018541	58.2775693	30.2267934	0.749860339	13.9414821
DTCWT	4.60514969	28.5305252	53.4321157	30.5123766	0.731588974	14.3882836
CVT	4.96744813	28.5305252	53.2214960	30.4792547	0.72253315	14.7817404
NSCT	4.05981452	28.5305252	51.4386793	30.4452571	0.734618554	14.2478112
NSCT-SR	4.07744035	29.2814062	59.2546759	30.5960216	0.753037937	14.3404974
<b>Proposed Method</b>	<b>5.18322270</b>	<b>28.8770032</b>	<b>60.5941442</b>	<b>33.3204827</b>	<b>0.913899674</b>	<b>20.5085906</b>

**Table 3:** Statistical measures of medical images (MR - PD / MR - T2) using different fusion algorithms

Algorithm	IE	API	SD	SF	Q <sup>AB/F</sup>	AG
SR	4.12114884	31.2894363	58.4680421	31.3952432	0.666062059	14.9793517
DTCWT	5.11378273	35.7291564	59.0671526	33.8828081	0.608331539	16.7578366
CVT	5.37379756	35.7291564	59.0080854	33.6761898	0.572363234	17.3735133
NSCT	4.76502047	35.7291564	56.8547955	34.6382756	0.657430519	16.7774680
NSCT-SR	4.65633174	35.3074665	64.5771954	34.8403822	0.672057027	16.8139816
<b>Proposed Method</b>	<b>5.76825510</b>	<b>42.5777819</b>	<b>72.3746702</b>	<b>42.0720571</b>	<b>0.768891429</b>	<b>29.7488215</b>

**Table 4:** Statistical measures of medical images (MR - T1 / MR - T2) using different fusion algorithms

Algorithm	IE	API	SD	SF	Q <sup>AB/F</sup>	AG
SR	4.10369391	39.7439747	54.3896434	20.1701504	0.700576382	8.58060435
DTCWT	4.09409023	38.4872207	50.6806919	18.5538621	0.6319296	7.73455388
CVT	4.19852037	38.4872207	50.5958384	18.4461995	0.607435852	7.90264034
NSCT	4.15122189	38.4872207	54.1300050	22.3373947	0.703388423	9.62983154
NSCT-SR	4.14119897	39.3973685	56.4339275	22.3963037	0.712289697	9.65765666
<b>Proposed Method</b>	<b>5.26167154</b>	<b>38.5832136</b>	<b>59.0750965</b>	<b>25.7096320</b>	<b>0.859418326</b>	<b>15.9817401</b>

**Table 5:** Statistical measures of medical images (MR - PD / MR - T2) using different fusion algorithm

## 5. Conclusion

NSCT-SR-FP (Nonsubsampled Contourlet Transform with Sparse Representation in Frequency Partition Domain) technique was proposed and applied to medical image fusion. Many more methods have been developed using SR, DTCWT, CVT, NSCT, NSCT-SR, and NSCT-SR in FP and compared. In order to check the reliability of the medical images, different quality assurance approaches are evaluated. The proposed NSCT-SR in FP shows better performance assessment metrics, which in turn has better image quality without any information loss or objects, among the various techniques applied to different pairs of medical images.

## References

1. Varsheny, P.K. Multisensor data fusion. *Elec. Comm. Eng. J.*, 1997, 9(12), 245-53.
2. Blum, Rick, S. & Liu, Zheng. *Multi-sensor image fusion and its applications*. Taylor & Francis Group, CRC Press, NW, 2006
3. Gonzalez, R.C. & Wintz, P. *Digital image processing*. Addison-Wesley, MA, 1987
4. Rama Mohan, Dr. S. Kiran, and R. Pradeep Kumar Reddy, A Study on Several Image Synthesis Algorithms, *Int. J. Information Technology and Computer Science Perspectives*, Pezzottaite Journals, 4(3) (2015), 1600-1608.
5. VPS Naidu, Discrete Cosine Transform based Image Fusion Techniques, *J. Communication, Navigation and Signal Processing*, 1(1)(2012), 35-45.
6. VPS Naidu, Block DCT based Image Fusion Techniques, *e-Journal of Science and Technology*, 49-66.
7. Veerpal Kaur, and Jaspreet Kaur, Frequency Partitioning Based Image Fusion for CCTV, *Int. J. Computer Science and Information Technologies*, 6 (4) (2015), 3968-3972.
8. VPS Naidu, and Bindu Elias, A Novel Image Fusion Technique using DCT based Laplacian Pyramid, *Int. J. Inventive Engineering and Sciences*, 1(2) (2013).
9. VPS Naidu, Multi Focus Image Fusion using the Measure of Focus, *J. Optics*, published by Springer, (2012).
10. VPS Naidu, Novel Image Fusion Techniques using DCT, *Int. J. Computer Science and Business Informatics*, 5(1) (2013).
11. Mohan C.R., and Kiran S. Image Enrichment Using Single Discrete Wavelet Transform Multi-resolution and Frequency Partition, *Artificial Intelligence and Evolutionary Computations in Engineering Systems, Advanced in Intelligent Systems and Computing*, Springer, 668.
12. Jingming Xia, Yiming Chen, Aiyue Chen, and Yicai Chen, Medical Image Fusion Based on Sparse Representation

- and PCNN in NSCT Domain, Computational and Mathematical Methods in Medicine, (2018).
13. Yin Fei, Gao Wei, and Song Zongxi, Medical Image Fusion Based on Feature Extraction and Sparse Representation, International Journal of Biomedical Imaging, (2017).
  14. S.Zhao-yu, H.Rong, and O.Ning, Image fusion based on multi-scale sparse representation, Computer Engineering and Design, 36(1) (2015).
  15. T. Guha and R. K. Ward, Learning sparse representations for human action recognition, IEEE Transactions on Pattern Analysis and Machine Intelligence, 34(8) (2012).
  16. S. T. Li, H. T. Yin, and L. Y. Fang, Group-sparse representation with dictionary learning for medical image denoising and fusion, IEEE Transactions on Biomedical Engineering, 59(12) (2012).
  17. Y. Liu, S. Liu, and Z. F. Wang, Medical image fusion by combining non sub sampled contourlet transform and sparse representation, Communications in Computer and Information Science, Pattern Recognition, Springer, 484, (2014).
  18. H. Yin, S. Li, and L. Fang, Simultaneous image fusion and super-resolution using sparse representation, Information Fusion, 14(3) (2013).
  19. C. M. Falco, X. Jiang, F. Yin, W. Gao, and Z. Song, Image fusion based on group sparse representation, in Proceedings of the Eighth International Conference on Digital Image Processing (ICDIP '16), Chengdu, China, August 2016.
  20. J. Wang, J. Peng, X. Feng, G. He, J. Wu, and K. Yan, Image fusion with nonsubsampling contourlet transform and sparse representation, Journal of Electronic Imaging, 22(4) (2013).
  21. Q. H. Zhang, Y. L. Fu, H. F. Li, and J. Zou, Dictionary learning method for joint sparse representation-based image fusion, Optical Engineering, 52(5) (2013).
  22. P. Jagalingam, and A.V. Hegde, A Review of Quality Metrics for Fused Image, Elsevier Transaction, Aquatic Procedia, 4 (2015), 133-142.
  23. Betsy Samuel, and Vidya N, Full Reference Image Quality Assessment for Biometric Detection, Int. J. Modern Trends in Engineering and Research, 02 (06) (2015).
  24. Mayuresh Gulame, K.R. Joshi, and Kamthe R.S, A Full Reference Based Objective Image Quality Assessment, Int. J. Advanced Electrical and Electronics Engineering, 2(6) (2013).
  25. Ratchakit Sakuldee, and Somkait Udomhunsakul, Objective Performance of Compressed Image Quality Assessments, Int. J. Computer and Information Engineering, 1 (2007).